

## Change in Mn 3d orbital state related to a metal-insulator transition in a bilayer manganite studied by magnetic Compton profile measurement

A. Koizumi,<sup>1,\*</sup> T. Nagao,<sup>1</sup> Y. Kakutani,<sup>1</sup> N. Sakai,<sup>1</sup> K. Hirota,<sup>2</sup> and Y. Murakami<sup>2,3</sup>

<sup>1</sup>Graduate School and Faculty of Science, Himeji Institute of Technology, Kamigori, Ako-gun, Hyogo 678-1297, Japan

<sup>2</sup>Department of Physics, Tohoku University, Sendai, Miyagi 980-8578, Japan

<sup>3</sup>Synchrotron Radiation Research Center, Japan Atomic Energy Research Institute (SPring-8), Mikazuki, Hyogo 679-5148, Japan

(Received 8 September 2003; published 10 February 2004)

Temperature dependence of magnetic Compton profile (MCP) has been measured on a single crystal of  $\text{La}_{2-2x}\text{Sr}_{1+2x}\text{Mn}_2\text{O}_7$  at  $x=0.42$  along the  $c$ -axis. The spin magnetic moments of Mn 3d electrons in  $t_{2g}$  and  $e_g$  type orbitals are evaluated from the line-shape fitting analysis of MCP's using theoretical profiles derived from the  $(\text{MnO}_6)^{8-}$  *ab initio* calculations. The experimental ratios of  $e_g$  spins to  $t_{2g}$  ones show higher values above the metal-insulator transition temperature  $T_c$  in comparison with the value expected from the electronically homogeneous state. This is understood in terms of the phase separation between electron-rich ferromagnetic and electron-poor antiferromagnetic regions. The ratios indicate that the  $e_g$  electrons are highly segregated in the ferromagnetic region. In addition, the fitting result just above  $T_c$  suggests that the  $e_g$ -orbital state involved with the colossal magnetoresistance effect is optimized by an external magnetic field.

DOI: 10.1103/PhysRevB.69.060401

PACS number(s): 75.25.+z, 71.30.+h, 71.38.-k, 75.47.Gk

Perovskite Mn oxides have provided a fascinating subject such as colossal magnetoresistance (CMR) observed just around a metal-insulator transition temperature  $T_c$ ,<sup>1-4</sup> where the charge, spin, and orbital degrees of freedom are arguably connected with each other. The ferromagnetism and metallic conductivity concurrently appeared below  $T_c$  have been understood on the basis of the double-exchange (DE) mechanism, where  $e_g$  electrons hop around Mn sites through hybridization with O-2p orbitals, and align the localized  $t_{2g}$  spins by the strong Hund's coupling.<sup>5-7</sup> However, the transport properties including CMR and the complicated magnetic phase diagrams of manganites cannot be explained by the simple DE mechanism, and some additional ingredient is required. It is currently pointed out that the lattice degree of freedom, which is strongly coupled with the orbital degree of freedom, plays an important role in understanding the physical properties of manganites.<sup>8-12</sup> Recent x-ray and neutron-scattering experiments have observed a short-range charge ordering (SRCO) within  $\text{MnO}_2$  layers, suggesting the localization of  $e_g$  electrons at Mn sites accompanied by local lattice distortions.<sup>13-16</sup> Kubota *et al.* have reported that in bilayer manganites, SRCO appears in the wide range of hole concentration and is characterized by a bistrife order running along the [100] direction in a  $\text{MnO}_2$  layer which forms streaks of two large and one small lattice distortions around  $\text{Mn}^{3+}$  and  $\text{Mn}^{4+}$  ions, respectively.<sup>15,16</sup> The temperature dependence of SRCO shows a notable change in the vicinity of  $T_c$ , and well corresponds to that of resistivity.<sup>15</sup> Therefore, determination of the electronic and orbital states around  $T_c$ , which are sensitive to the local structural change, will provide a clue to elucidate the mechanism of CMR.

Our previous paper demonstrated that magnetic Compton-profile (MCP) measurement is capable of determining the population of Mn-3d orbitals which hybridize with O-2p orbitals.<sup>17</sup> In the present study, we have measured the temperature dependence of MCP on a bilayer manganite, and made a line-shape analysis on MCP's using theoretical pro-

files of  $e_g$  and  $t_{2g}$  type orbitals. From the analytical results, we will discuss the change in  $e_g$  electron density depending on temperature and the effect of magnetic field on the  $e_g$ -orbital state just above  $T_c$ .

The MCP,  $J_{\text{mag}}(p_z)$ , is defined as the double integral of the difference in momentum density between spin-up and spin-down electrons with respect to  $p_x$  and  $p_y$ ,

$$J_{\text{mag}}(p_z) = \int \left( \sum_i |\phi_{i\uparrow}(\mathbf{p})|^2 - \sum_j |\phi_{j\downarrow}(\mathbf{p})|^2 \right) dp_x dp_y, \quad (1)$$

where  $p_z$  is an electron-momentum component along the direction of the scattering vector of x rays. The  $\phi_{i\sigma}(\mathbf{p})$  is a wave function in momentum space, and  $|\phi_{i\sigma}(\mathbf{p})|^2$  means the momentum density of  $i$ th state. The subscript  $i$  and  $j$  go through all occupied spin-up and spin-down states, respectively. The MCP is sensitive only to the spin magnetic moment,<sup>18</sup> and its area is proportional to the magnitude of spin magnetic moment. In addition, the MCP measurement is advantageous to the study of orbital states, because the shape of MCP varies according to orbitals occupied by magnetic electrons. This feature enables us to separately determine the spin magnetic moments in  $e_g$  and  $t_{2g}$  type orbitals on manganites based on the theoretical profiles of them.<sup>17</sup>

The sample was a single crystal of bilayer manganite  $\text{La}_{2-2x}\text{Sr}_{1+2x}\text{Mn}_2\text{O}_7$  at  $x=0.42$ , which was melt-grown in flowing oxygen gas in a floating zone optical image furnace.<sup>19</sup> This system shows two-dimensional conductivity, because a pair of  $\text{MnO}_2$  layers is interlaced between two  $(\text{La}, \text{Sr})_2\text{O}_2$  blocking layers. According to the magnetic phase diagram obtained by neutron-diffraction measurement,<sup>20</sup> the magnetic structure of the present sample is canted antiferromagnetic (canted AFM) below  $T_c$ , where the magnetic moments in a  $\text{MnO}_2$  layer are ferromagnetically aligned and slightly canted between the two layers within a bilayer. Above  $T_c$ , the sample changes to AFM-I insulator phase, where the magnetic moments are antiferro-

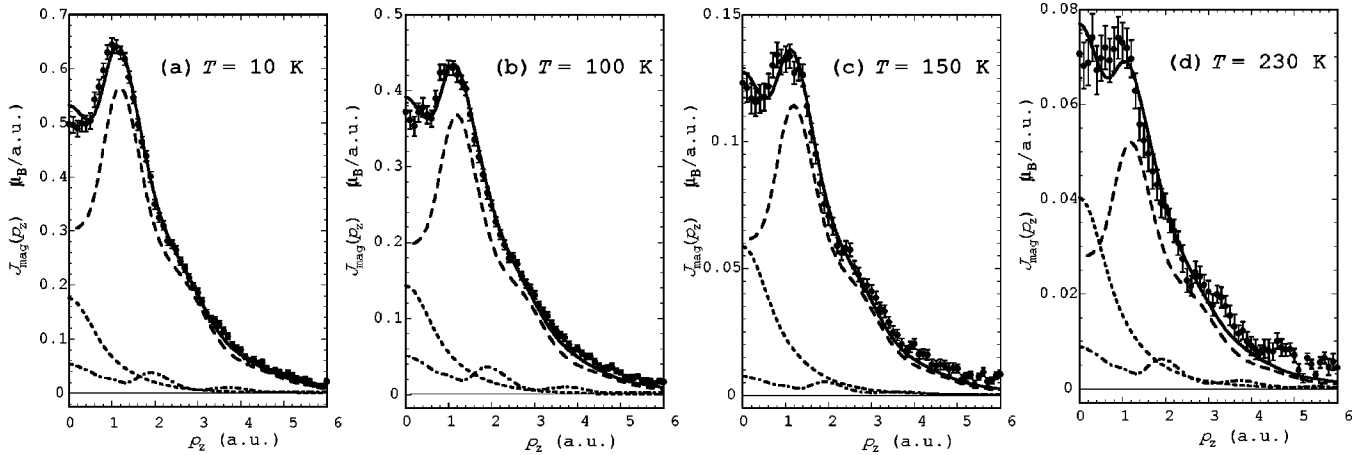


FIG. 1. The magnetic Compton profiles along the  $c$ -axis measured at (a) 10 K, (b) 100 K, (c) 150 K, and (d) 230 K under the external field of  $\pm 2.5$  T. The abscissa represents an electron momentum  $p_z$  in the atomic unit (a.u.). Experimental data (solid circles) are shown with fit (solid line) using the  $\text{MnO}_6$  cluster orbitals. Error bars indicate experimental statistical errors. The  $t_{2g}$ ,  $e_{x^2-y^2}$ , and  $e_{3z^2-r^2}$  type orbital contributions are denoted by dashed, dotted, and dotted-dashed lines, respectively (Ref. 21).

magnetically ordered between the two layers, and the CMR is observed in this phase. The sample becomes paramagnetic (PM) above 170 K. We measured the magnetic susceptibility on the sample and determined  $T_c$  to be 95 K.

MCP measurements were made at 10, 100, 150, and 230 K on the beamline 08W at SPring-8, Japan. Circularly polarized x rays emitted from an elliptical multipole wiggler were monochromatized to 174 keV and incident on the sample. The Compton scattered x rays with a scattering angle of  $178.5^\circ$  were energy analyzed by a 10-segmented Ge solid-state detector. During the measurement, an external magnetic field of  $\pm 2.5$  T was alternatively applied along the  $c$ -axis of the sample to reverse the magnetization direction. Each MCP was extracted as the difference between two measured Compton profiles of the sample magnetized mutually in the opposite directions with a fixed photon polarization. The MCP's above  $T_c$  were measured on the sample with field-induced magnetization. Then, the orbital state on the condition of CMR will be reflected in the MCP particularly at 100 K.

The MCP's obtained are shown in Fig. 1. The area of each MCP is normalized to the corresponding magnetization listed

in Table I. It is noticed that the dip in the low momentum region,  $p_z < 1.0$  a.u., becomes shallower with increasing temperature. We can qualitatively examine the change of MCP's with atomic profiles of  $e_g$  and  $t_{2g}$  orbitals, since the magnetization of manganite is induced by the spins in Mn-3d orbitals. The result suggests that the ratio of  $e_g$  spin magnetic moments to  $t_{2g}$  ones increases above  $T_c$ , because the atomic  $e_g$ -orbital profile shows a peak at  $p_z = 0$ , while  $t_{2g}$ -one has a dent. To quantitatively evaluate the spin magnetic moments in respective orbitals, the fitting analysis of each MCP has been carried out using theoretical profiles of  $t_{2g}$ ,  $e_{x^2-y^2}$ , and  $e_{3z^2-r^2}$  type orbitals obtained from an *ab initio* molecular orbital calculation for a  $(\text{MnO}_6)^{8-}$  cluster which takes the hybridization effect between Mn-3d and O-2p orbitals into account.<sup>21</sup> The  $z$ -axis is taken to be parallel to the  $c$ -axis. The  $t_{2g}$  profile is treated as the sum of  $xy$ ,  $yz$  and  $zx$  orbitals because those orbitals are considered to be fully occupied. The details of the calculation are described in Ref. 17. The fitting results are shown by the lines in Fig. 1 and listed in Table I.

In the case of manganites, it is reasonable to consider that the occupation number in each Mn-3d orbital is proportional

TABLE I. Spin magnetic moments in respective orbitals evaluated from the fitting analysis of MCP. Each value is normalized by the magnetic moment per Mn site,  $M(\mu_B/\text{Mn})$ , obtained by magnetization measurement at the field of 2.5 T. The results at 150 and 230 K are shown in a large number of decimals, which is due to the small normalization factor,  $M$ . The  $e_g/t_{2g}$  and  $e_{3z^2-r^2}/e_{x^2-y^2}$  mean the ratios of  $e_g$  to  $t_{2g}$  and  $e_{3z^2-r^2}$  to  $e_{x^2-y^2}$  spin magnetic moments, respectively.

$T(\text{K})$	$M(\mu_B/\text{Mn})$	$t_{2g}$	$e_{x^2-y^2}$	$e_{3z^2-r^2}$	$e_g/t_{2g}$	$e_{3z^2-r^2}/e_{x^2-y^2}$
10	3.12	2.49 ( $\pm 0.03$ )	0.37 ( $\pm 0.02$ )	0.21 ( $\pm 0.03$ )	0.23	0.57
100	2.20	1.62 ( $\pm 0.02$ )	0.30 ( $\pm 0.02$ )	0.20 ( $\pm 0.03$ )	0.31	0.67
150	0.69	0.503 ( $\pm 0.011$ )	0.124 ( $\pm 0.007$ )	0.030 ( $\pm 0.013$ )	0.31	0.24
230	0.38	0.229 ( $\pm 0.009$ )	0.085 ( $\pm 0.006$ )	0.035 ( $\pm 0.011$ )	0.52	0.41

to the spin moment evaluated from the analysis of MCP, since the strong Hund's coupling works between  $t_{2g}$  and  $e_g$  spins. If the area of MCP is normalized to 3.58, i.e., the nominal 3d electron number for  $x=0.42$ , the orbital populations at 10 K are given as 2.86, 0.43, and 0.24 for  $t_{2g}$ ,  $e_{x^2-y^2}$ , and  $e_{3z^2-r^2}$  type orbitals, respectively, which are in good agreement with the previous result.<sup>17</sup> If the sample is electronically homogeneous, the ratio  $e_g/t_{2g}$  in the present sample is expected to be 0.193 on the assumption that the  $t_{2g}$  and  $e_g$  populations are 3 and 0.58, respectively. Here the  $e_g$  contribution is the sum of  $e_{x^2-y^2}$  and  $e_{3z^2-r^2}$  orbital populations. In the canted AFM region below  $T_c$ , the experimental ratio at 10 K deduced from the fitting results shows 0.23 that is slightly larger than the expected ratio. It is to be anticipated that in AFM-I phase, both the ratios at 100 and 150 K give a significantly large value of 0.31. The ratio at 230 K in PM phase shows an even larger value of 0.52, although it is less reliable because the measurement was made on the sample with field-induced weak magnetization resulting in poor statistics. Since the MCP measurement detects the only ferromagnetic (FM) component in the sample and does not the AFM one, these results mean that the density of  $e_g$  electrons is high in the observed FM state and the electronic inhomogeneity of the sample is remarkable particularly above  $T_c$ , and suggest the concomitance of  $e_g$ -electron poor AFM state. Yunoki *et al.* have theoretically predicted the phase separation (PS) between the electron-rich FM and the electron-undoped AFM regions in the high hole doping level.<sup>22-26</sup> According to this description, the increase in  $e_g/t_{2g}$  can be understood as a result of decrease in  $t_{2g}$  spin contribution to MCP. That is, in the AFM region with no  $e_g$  electrons,  $t_{2g}$  spin moments cancel each other and do not contribute to MCP. The ratio will therefore become large, if all the  $e_g$  electrons are in the FM region. The volume fraction of the FM region may be given by  $M(T)/3.58$  below and just above  $T_c$ , because the thermal fluctuation of magnetic moments would be small at these temperatures. In practice, the ratios at 10 and 100 K are well explained by  $0.193 \times 3.58/M(T)$ . Specifically, the ratio of 0.31 at 100 K is possible when about three fifth parts of the sample is the electron-rich FM region, and the rest is the electron-undoped AFM region. However, large FM domains with high electron density could not exist because of the charge neutrality. It should be divided into small clusters. In fact, several experiments have observed magnetic clusters above  $T_c$ .<sup>27-29</sup> Small-angle neutron scattering (SANS) measurement has shown that the magnetic correlation length, which provides the size of the clusters, is of the order of a few lattice spacing, and rapidly diverges below  $T_c$ . In manganite, the factor contributing to the ferromagnetic small clusters would be underlying in the form of charge-segregated domains, which may originate in the local chemical and structural inhomogeneity.<sup>30</sup> On the other hand, SRCO, which is associated with the localization of  $e_g$  electrons, disappears below  $T_c$ . The above ratios therefore, indicate that the electronic state is comparatively homogeneous below  $T_c$ , while the  $e_g$  electrons are highly segregated in the magnetic clusters above  $T_c$ , and the degree of charge segregation varies according to the magnetic phases such as canted AFM, AMF-I,

and PM states. In this regard, the PS observed in the present study would depend on temperature.

Another significant finding is the effect of external field on the  $e_g$  orbital state just above  $T_c$ . The  $e_g$  orbital state at 100 K shows a high proportion of  $e_{3z^2-r^2}$  component in comparison with that at 150 K, although the ratio  $e_g/t_{2g}$  is almost the same at both temperatures. The ratio of  $e_{3z^2-r^2}$  to  $e_{x^2-y^2}$  spin moments makes this aspect clear as listed in Table I. The  $e_{3z^2-r^2}/e_{x^2-y^2}$  at 100 K is larger than the ratio at 150 K, and shows a comparable value to the ratio at 10 K. This means that the  $e_g$  state at 150 K is dominated by the  $x^2-y^2$  orbital character, and the  $e_g$ -orbital configuration at 100 K, just above  $T_c$ , is similar to that at 10 K under the present external field.

In zero-magnetic field, the electronic state above  $T_c$  would be a polaronic state with highly localized  $e_g$  electrons, specifically the  $e_{x^2-y^2}$  electrons at least in a high hole doping region. In fact, the above result at 150 K, where the CMR effect becomes small, is consistent with this view, and well describes the AFM-I phase, i.e., the low population of  $3z^2-r^2$  orbital weakens the interlayer ferromagnetic coupling within a bilayer. Then, the superexchange antiferromagnetic coupling between  $t_{2g}$  orbitals overcomes the DE interaction along the  $c$ -axis. Consequently, the system is in AFM-I phase. The dominance of  $x^2-y^2$  orbital is also supported by the fact that in bilayer manganite at  $x=0.4$ , the Jahn-Teller distortion measured by a neutron diffraction experiment becomes small around  $T_c$ .<sup>31</sup> Such relaxation of lattice distortion will work for the stabilization of  $x^2-y^2$  orbital. Hence, the  $\text{MnO}_2$  layers in the charge-segregated domain would be substantially filled with  $e_{x^2-y^2}$  electrons, because the ratio  $e_g/t_{2g}$  of 0.31 at 100 K implies that the density of  $e_g$  electrons is about 1.6 times higher in the magnetic clusters just above  $T_c$  than in the electronically homogeneous state. In such a situation, the  $e_{x^2-y^2}$  electrons may be immobilized by the electron correlation between them, resulting in insulating. This is likely to be related to SRCO with local lattice distortion which will affect on the  $e_g$  orbital state. A neutron diffraction study has found that an applied magnetic field causes the collapse of SRCO,<sup>14</sup> while both SANS and emission Mössbauer studies have reported that above  $T_c$ , the magnetic clusters grow in size on application of a magnetic field.<sup>27,29</sup> These observations suggest that the percolative network of magnetic clusters, which will be a requirement for CMR, expands with decreasing SRCO. In addition to this, the ratio  $e_{3z^2-r^2}/e_{x^2-y^2}$  at 100 K indicates that the change in  $e_g$  orbital state by an external field interprets the CMR phenomenon; the applied field aligns the Mn magnetic moments of the magnetic clusters. As shown by the ratio  $e_{3z^2-r^2}/e_{x^2-y^2}$  at 100 K, some of the localized  $e_{x^2-y^2}$  electrons move into the  $3z^2-r^2$  orbitals in the combined magnetic clusters, which will play a part in the relaxation of local lattice distortion. The change in orbital configuration will simultaneously induce sufficient holes in the  $\text{MnO}_2$  layer dominated by  $e_{x^2-y^2}$  electrons. The holes correspond to the amount of  $e_g$  electrons transferred from  $x^2-y^2$  to  $3z^2-r^2$  orbital. This will effectively activate the DE interaction in the system, and metallic conductivity will be brought back in

the  $\text{MnO}_2$  layer, thus CMR. The stabilization of  $3z^2-r^2$  orbital will also facilitate conductivity along the  $c$ -axis and the ferromagnetic coupling between the two layers within a bilayer, and will come along with an elongation of the bond length between Mn and apical O. Indeed, the fitting result at 100 K is consistent with a large magnetostriction around  $T_c$  observed in the bilayer manganite at  $x=0.4$ ,<sup>32</sup> and therefore indicates that the  $e_g$ -orbital state on the condition of CMR is optimized by external fields.

In summary, we have measured the temperature dependence of MCP for  $\text{La}_{2-2x}\text{Sr}_{1+2x}\text{Mn}_2\text{O}_7$  at  $x=0.42$  along the  $c$ -axis. The values of spin magnetic moments of  $t_{2g}$  and two  $e_g$  ( $e_{x^2-y^2}$  and  $e_{3z^2-r^2}$ ) type orbitals are obtained by the fitting analysis of each MCP using theoretical profiles derived from the  $(\text{MnO}_6)^{8-}$  cluster calculation. The ratio of  $e_g$  to  $t_{2g}$  spin magnetic moments shows higher values above  $T_c$  than at 10 K. This is explained in terms of the phase separation between electron-rich FM and electron-undoped AMF regions. The ratios indicate that the  $e_g$  electrons are highly segregated in the magnetic clusters above  $T_c$ , and such elec-

tronic state with high density of  $e_g$  electrons exists as an underlying factor for CMR. In addition, the ratio of  $e_{3z^2-r^2}$  to  $e_{x^2-y^2}$  spin moments at 100 K suggests that the change in  $e_g$ -orbital state by external fields plays an important role in the CMR phenomenon in manganites. The  $e_g$ -orbital state around  $T_c$  may change according to the strength and the direction of applied fields. The field dependence of MCP will be able to verify the change in  $e_g$  orbital state. Measurements of anisotropy in MCP will be also effective to clarify the influence of the external field on the  $e_g$  orbital state around  $T_c$ , because MCP of each orbital changes its shape depending also on the direction of observation.

We are indebted to Dr. Y. Sakurai and Dr. M. Ito for their help with the MCP measurements. We also thank Dr. H. Koizumi and Dr. M. Kubota for useful discussions. The synchrotron radiation experiments were performed with the approval of the Japan Synchrotron Radiation Research Institute (JASRI) (Proposal No. 2002A0008-LD3-np). This work was supported by a Grant-In-Aid for Science and Culture, Japan.

\*Electronic address: akihisa@sci.himeji-tech.ac.jp

<sup>1</sup>R. von Helmolt *et al.*, Phys. Rev. Lett. **71**, 2331 (1993).

<sup>2</sup>S. Jin *et al.*, Science **264**, 413 (1994).

<sup>3</sup>A. Urushibara *et al.*, Phys. Rev. B **51**, 14 103 (1995).

<sup>4</sup>Y. Moritomo *et al.*, Nature (London) **380**, 141 (1996).

<sup>5</sup>C. Zener, Phys. Rev. **82**, 403 (1951).

<sup>6</sup>P.W. Anderson and H. Hasegawa, Phys. Rev. **100**, 675 (1995).

<sup>7</sup>P.G. de Gennes, Phys. Rev. **118**, 141 (1960).

<sup>8</sup>A.J. Millis *et al.*, Phys. Rev. Lett. **74**, 5144 (1995).

<sup>9</sup>H. Röder *et al.*, Phys. Rev. Lett. **76**, 1356 (1996).

<sup>10</sup>A.J. Millis *et al.*, Phys. Rev. Lett. **77**, 175 (1996).

<sup>11</sup>D. Louca *et al.*, Phys. Rev. B **56**, R8475 (1997).

<sup>12</sup>H. Koizumi *et al.*, Phys. Rev. Lett. **80**, 4518 (1998).

<sup>13</sup>S. Shimomura *et al.*, Phys. Rev. Lett. **83**, 4389 (1999).

<sup>14</sup>L. Vasiliiu-Doloc *et al.*, Phys. Rev. Lett. **83**, 4393 (1999).

<sup>15</sup>M. Kubota *et al.*, J. Phys. Soc. Jpn. **69**, 1986 (2000).

<sup>16</sup>M. Kubota *et al.*, J. Phys. Soc. Jpn. **70**, 91 (2001).

<sup>17</sup>A. Koizumi *et al.*, Phys. Rev. Lett. **86**, 5589 (2001).

<sup>18</sup>N. Sakai, J. Phys. Soc. Jpn. **63**, 4655 (1994).

<sup>19</sup>K. Hirota *et al.*, J. Phys. Soc. Jpn. **67**, 3380 (1998).

<sup>20</sup>M. Kubota *et al.*, J. Phys. Chem. Solids **60**, 1161 (1999).

<sup>21</sup>In this report, we use  $e_{x^2-y^2}$  and  $e_{3z^2-r^2}$  to denote  $x^2-y^2$  and  $3z^2-r^2$  type orbitals of the  $e_g$  state, respectively.

<sup>22</sup>S. Yunoki *et al.*, Phys. Rev. Lett. **80**, 845 (1998).

<sup>23</sup>S. Yunoki and A. Moreo, Phys. Rev. B **58**, 6403 (1998).

<sup>24</sup>E. Dagotto *et al.*, Phys. Rev. B **58**, 6414 (1998).

<sup>25</sup>S. Yunoki *et al.*, Phys. Rev. Lett. **81**, 5612 (1998).

<sup>26</sup>A. Moreo *et al.*, Science **283**, 2034 (1999).

<sup>27</sup>J.M. De Teresa *et al.*, Nature (London) **386**, 256 (1997).

<sup>28</sup>O. Chauvet *et al.*, Phys. Rev. Lett. **81**, 1102 (1998).

<sup>29</sup>V. Chechersky *et al.*, Phys. Rev. B **59**, 497 (1999).

<sup>30</sup>T. Shibata *et al.*, Phys. Rev. Lett. **88**, 207205 (2002).

<sup>31</sup>J.F. Mitchell *et al.*, Phys. Rev. B **55**, 63 (1997).

<sup>32</sup>T. Kimura *et al.*, Phys. Rev. Lett. **81**, 5920 (1998).